Joint Estimation of ToA and Data Symbols in UWB Communication in Presence of Impulsive Interference

Sanjeev Sharma[1], Anubha Gupta[2] (Senior Member, IEEE) and Vimal Bhatia[1] (Senior Member, IEEE)
[1] SaSg, Discipline of Electrical Engineering, Indian Institute of Technology Indore, India 453552 {phd1501102011,vbhatia}@iiti.ac.in
[2] SBILab, Department of Electronics and Communication Engg., IIIT-Delhi, New Delhi-110020, anubha@iiitd.ac.in

***Abstract*—Ultra-wide band (UWB) ranging requires precise estimation of time-of-arrival (ToA) of first path (FP) signal. In UWB communication, estimation of ToA is challenging in the presence of impulsive interference and multipath. Generally in literature, ToA is estimated using threshold crossing techniques. Although threshold based ToA methods are simple, optimal threshold value is hard to determine in practice. In this paper, we propose joint estimation of ToA and data symbols by exploiting the cluster-sparsity of the received UWB signal in the presence of impulsive interference. The proposed receiver structure enhances the signal-to-noise ratio at the receiver output by mitigating the impulsive interference and barring inter-clusters noise accumulation. The proposed method is also free from any threshold, training, and optimization process. Robustness of the proposed algorithm is validated for standardized IEEE 802.15.4a channel models in the presence of both additive white Gaussian noise and impulsive interference.**

***Index Terms*—cluster-sparsity, impulsive interference, multipath, threshold, ToA of first path, UWB ranging and communication.**

I. Introduction

Ultra-wide band (UWB) ranging requires precise estimation of time-of-arrival (ToA) of the first path (FP) [1] that is generally referred to as ToA estimation. The coherent detection based ToA estimation methods [1–3] have better performance. However, coherent receivers have higher system implementation complexity. Low complexity non-coherent receivers for UWB ranging have also been analyzed in the literature, specially for Wireless Sensor Networks (WSNs) and Internet of Things (IoT) applications. In [4–7], ToA is estimated using the time index of the first threshold crossing (TC) of the received signal. TC based ToA methods are simple. However, they need a precise value of the threshold, which is hard to obtain in practice. ToA can also be estimated using the maximum energy path (MEP) criteria, however FP is not always the MEP. Hence, the existing MEP based ToA generally leads to large errors in FP estimation [7]. In [1, 5, 7], MEP estimation with backward search procedure is suggested. However, this also requires optimal value of the threshold. TC based ToA estimation methods are sensitive to noise and interference because TC is determined using the bin energy. Also, the accuracy of TC based UWB ranging is limited by the bin size. Hence, both these drawbacks are required to be addressed in UWB applications. Further, the estimation of ToA is also proposed using information theoretic criteria without the need of any threshold [8]. However, proposed method in [8], may not be suitable for highly dynamic and interference environment.

The low power UWB signals experience impulsive interference either from multiuser interference (MUI) or from surrounding physical noise sources or from radio frequency interference such as narrowband communication [2, 4, 9–14]. Due to impulsive interference, FP of the desired signal is either suppressed or wrongly estimated at the receiver. This degrades the accuracy of the UWB ranging. Alternatively, there are non-linear processing techniques such as limiter and blanking, that improve robustness of a receiver in impulsive interference [9, 11, 15, 16]. However, they require exact estimation of signal and noise statistics for the selection of precise threshold value, which is difficult to obtain in a practical scenario [4]. In the literature [2, 6–8, 13], most of the ToA estimation methods are analyzed assuming additive white Gaussian noise (AWGN) scenario in UWB ranging. Hence, the analysis of UWB ranging and its robustness is important in high impulsive interference environments such as in mining and industrial units.

We propose a non-coherent UWB receiver that jointly estimates the ToA and data symbols using the cluster-sparsity of the received UWB signal, in the presence of both impulsive interference and Gaussian noise. In the proposed receiver, first impulsive interference is mitigated (using the proposed cluster detection algorithm), then the received signal is processed for ToA and data symbols estimation using the proposed cluster finding algorithm (CFA). The proposed receiver does not require any training phase, optimization process, and threshold. Further, the channel and noise patterns are unknown at the receiver. The validity of the proposed receiver is demonstrated in time-hopping (TH) binary pulse position modulation (BPPM) UWB system using standard IEEE 802.15.4a channel models in the presence of both impulsive interference and AWGN. Performance of the proposed receiver has also been compared with the TC based ToA estimation methods.

Rest of the paper is organized as follows: In Section II, TH-BPPM UWB system model is described in the presence of impulsive interference. A non-coherent receiver for joint estimation of ToA and data symbols is proposed in Section III. This Section also proposes impulsive interference mitigation technique using the cluster-sparsity of the UWB signal.

Numerical results and discussion are presented in Section IV. Conclusions are drawn in Section V.

Notations: $\mathcal{N}(\nu, \sigma^2)$ represents the Gaussian probability distribution function (pdf) with mean ν and variance σ^2. $\lfloor(\cdot)\rfloor$ and $|(\cdot)|$ denote the floor function and absolute magnitude value of $(\cdot)$, respectively. $\|(\cdot)\|_2$ is the Euclidian norm of a signal $(\cdot)$ and $Pr\{\mathcal{B}\}$ denotes the probability of event $\mathcal{B}$. $Q(\cdot)$ is the Q-function and is expressed as $Q(x) = 1/\sqrt{2\pi}\int_x^\infty \exp(-x^2/2)dx$.

II. System Model

In UWB system, each data symbol is transmitted using N_f consecutive frames and each frame has a single pulse. The composite signal $s_c(t)$ of N_f frames using pulse $p(t)$ of time duration T_p is written as

$$s_c(t) = \sqrt{\frac{E_p}{N_f}} \sum_{j=0}^{N_f-1} p(t - jT_f - c_j T_c),\ t \in \mathbb{R}, \tag{1}$$

where E_p ($E_p = \int_{t=-\infty}^{\infty} p(t)^2 dt$) and T_f are pulse energy and frame duration, respectively. $\{c_j\}$ is the TH code and T_c is the chip duration [11]. The received signal is expressed as

$$r(t) = \sum_{k=0}^{\infty} w_r(t - kT_s) + i_{\mathrm{mui}}(t) + i(t) + n(t), \tag{2}$$

where $w_r(t) = \sum_{l=0}^{L-1} \alpha_l s_c(t - d_k\Delta - \tau_l)$ and L denotes the total number of resolved multipaths in the channel impulse response (CIR). $\{\alpha_l\}_{l=1}^{L}$ and $\{\tau_l\}_{l=1}^{L}$ represent CIR's gain and delay parameters, respectively. $T_s = N_f T_f$ is the data symbol duration and $d_k \in \{0, 1\}$ denotes the k^{th} frame data symbol. The parameter Δ is the time shift in a frame for $d_k = 1$ and is called the PPM modulation index. $i(t)$ is Bernoulli-Gaussian (BG) impulse noise (IN) [9] of zero mean and σ_I^2 variance with occurrence probability of p in a given time duration. $i(t)$ models the sparsely occurring high amplitude outliers of the received signal that can occur due to hardware impairment or the surrounding IN sources. $n(t)$ is AWGN of zero mean and σ_n^2 variance, i.e., $n(t) \sim \mathcal{N}(0, \sigma_n^2)$. $i_{\mathrm{mui}}(t)$ represents MUI and is expressed as

$$i_{mui}(t) = \sum_{u=1}^{U} \sum_{k=0}^{\infty} w_{mui}^u(t - kT_s - \check{\tau}_u), \tag{3}$$

where $w_{mui}^u(t) = \sum_{l=0}^{L-1} \tilde{\alpha}_l^u s_c^u(t - d_k^u\Delta - \tilde{\tau}_l^u)$ and $\check{\tau}_u$ is the delay time of the u^{th} interferer at the receiver. $\{\tilde{\alpha}_l^u, \tilde{\tau}_l^u\}_{l=1}^{L}\ \forall\ u$ are channel parameters (gain and delay) and $d_k^u \in \{0, 1\}$ denotes data symbols of u^{th} interferer in the k^{th} frame. U is the total number of multiuser interferers in the system. Both $i_{\mathrm{mui}}(t)$ and $i(t)$, combined or individually, create impulsive interference in the system [9, 10, 17]. Each interferer has different TH code and arrival time at the receiver. Further, TH code of the desired user is known at the receiver with quasi-static CIR across N_f consecutive frames. Interferers' TH codes are unknown and CIRs are dynamic at the desired user's receiver. All interferers use the same (BPPM) modulation scheme and transmitted pulse. Further, signal-to-noise ratio (SNR), signal-to-impulse noise ratio (SIR), and effective SNR (ESNR) are expressed as SNR $= E_p/\sigma_n^2$, SIR $= E_p/\sigma_I^2$, ESNR $= E_p/(p\sigma_I^2 + \sigma_n^2 + \sigma_{\mathrm{mui}}^2)$, respectively, where σ_{mui}^2 is the variance of MUI. τ_1 represents the true ToA of FP of the desired user in the k^{th} frame and is required to be estimated from the received signal $r(t)$ in (2).

III. Proposed Receiver for Joint ToA and data symbols estimation

In this section, first we propose mitigation of impulsive interference from the received signal. Next, the joint estimation of TOA and data symbols are carried out using our recently proposed non-coherent receiver in [18]. The impulsive interference makes the estimation of ToA of the desired signal difficult due to FP suppression. Therefore, conventional energy detection (ED) based receiver's performance deteriorates and may have very high ranging and data symbols estimation error. Hence, it is essential to carry out mitigation of impulsive interference before the estimation of ToA. $\mathbf{r}$, $\mathbf{p}$, $\mathbf{i}_{\mathrm{mui}}$, $\mathbf{i}$, and $\mathbf{n}$ represent the received signal, transmitted pulse, MUI, impulse and Gaussian noises, respectively, corresponding to the analog counterpart at the Nyquist rate. The received signal is written as $\mathbf{r} = \mathbf{s} + \mathbf{i}_{mui} + \mathbf{i} + \mathbf{n} \in \mathbb{R}^N$, where $\mathbf{s}$ is the desired multipath UWB signal. Mitigation of impulsive interference (MUI and IN) from the received signal, and the cluster finding algorithm based ToA and data symbols estimation are described below.

A. IN detection and mitigation

In this subsection, a novel signal cluster detection algorithm (CDA) for IN detection and mitigation is proposed for the UWB receiver design. It is known that the UWB signal cluster is symmetric around the maximum absolute peak value of the transmitted pulse [9, 18, 19]. This cluster symmetry can be used to differentiate between the signal cluster and IN. Since the symmetry of UWB signal is observed irrespective of the type of transmitted pulse, the proposed method can be used for any UWB pulse shape.

The received signal $\mathbf{r}$ can be classified via two hypotheses, expressed as

$$\begin{aligned} \mathcal{H}_{\mathbf{i}} &: \mathbf{r} = \mathbf{s} + \mathbf{i}_{mui} + \mathbf{i} + \mathbf{n} \in \mathbb{R}^N, \\ \mathcal{H}_{\mathbf{s}} &: \mathbf{r} = \mathbf{s} + \mathbf{i}_{mui} + \mathbf{n} \in \mathbb{R}^N. \end{aligned} \tag{4}$$

$\mathbf{i}_{mui}$ has amplitude comparable to the desired signal $\mathbf{s}$, but is generally located at different time positions than the signal $\mathbf{s}$. The received signal $\mathbf{r}$ is the mixture of desired multipath UWB signal, MUI, and sparse IN. The maximum absolute value of $\mathbf{r}$ and its corresponding index are calculated and expressed as

$$[P_{max}^1, I_{max}^1] = \max(|\mathbf{r}|). \tag{5}$$

The sample $P_{\mathrm{max}}^1 = |\mathbf{r}(I_{\mathrm{max}}^1)|$ either belongs to hypothesis $\mathcal{H}_{\mathbf{s}}$ or to $\mathcal{H}_{\mathbf{i}}$. P_{max}^1 is classified using the apriori information of the UWB signal and that of IN. The UWB signal appears in the form of cluster, while IN is random in nature. We formed a contrived cluster centered at I_{max}^1 and express as $\mathbf{c}_{in} = \mathbf{r}(I_{max}^1 - M/2 : I_{max}^1 + M/2)$, where $(M+1)$ is the length of

UWB pulse. The Euclidean distance between contrived cluster $\mathbf{c}_{in}$ and UWB pulse is calculated as

$$d_{\mathbf{c}_{in},\mathbf{p}} = \sqrt{\sum_{n_m=1}^{M+1} \left(\mathbf{c}_{in}(n_m) - \mathbf{p}(n_m)\right)^2}. \quad (6)$$

By observing the $d_{\mathbf{c}_{in},\mathbf{p}}$, P^1_{max} is classified as

$$d_{\mathbf{c}_{in},\mathbf{p}} \underset{\mathcal{H}_\mathbf{s}}{\overset{\mathcal{H}_\mathbf{i}}{\gtrless}} \mu. \quad (7)$$

If $P^1_{max} \in \mathcal{H}_\mathbf{s}$, then $\mathbf{r}$ does not have IN and is further processed for MUI mitigation as shown in Fig. 1. However, if $P^1_{max} \notin \mathcal{H}_\mathbf{s}$, i.e., if $\mathbf{r}(I^1_{max}) \in \mathcal{H}_\mathbf{i}$, then the peak value $\mathbf{r}(I^1_{max})$ corresponds to IN and is assigned zero value. After removing $\mathbf{r}(I^1_{max})$ (if $P^1_{max} \in \mathcal{H}_\mathbf{i}$), signal is expressed as

$$\mathbf{r} = \mathbf{r} - \mathbf{e}_{I^1_{max}}\mathbf{r}, \quad (8)$$

where $\mathbf{e}_{I^1_{max}} \in \mathbb{R}^N$ and has one at $(I^1_{\max})^{\text{th}}$ position, while the remaining entries are zero. Again, the maximum absolute peak value of the above modified signal $\mathbf{r}$ (after assigning zero to impulse noise sample $\mathbf{r}(I^1_{max})$) is calculated and classified using (5), (6) and (7), respectively. This procedure is repeated until maximum absolute peak value of $\mathbf{r}$ does not belong to $\mathcal{H}_\mathbf{s}$. The proposed of CDA based IN detection and mitigation is also summarized in **Algorithm 1**. Further, the value of μ in (7) is selected using the transmitted pulse $\mathbf{p}$ and is expressed as $\mu \approx \|\mathbf{p}\|_2 \exp(1/\text{SNR (dB)})$, SNR (dB) > 0, where $\exp(\cdot)$ is the exponential function of $(\cdot)$. The parameter μ is approximated based on empirical results. As SNR increases, μ should decrease for better IN mitigation. Above value of μ provides good system performance. Hence, selection of μ is independent of IN parameters. The exact value of μ can be selected using the Bayesian estimation and left for the future work.

B. MUI mitigation

The MUI ($\mathbf{i}_{mui}$) mitigates using different TH codes of each interferer and be averaging over N_f frames (number of frames per data symbol). The multipath components (MPCs) of MUI are not aligned with the desired signal in time due to different TH. Over the N_f consecutive frames, the desired signal is similarly time-aligned. Hence, after averaging, MUI is mitigated (or minimized) without perturbing the desired signal. The signal corresponding to a data symbol in each frame is written as

$$\tilde{\mathbf{r}}_i = \tilde{\mathbf{r}}(1 + (i-1)\Lambda : i\Lambda), \quad i = 1, 2, ..., N_f, \quad (9)$$

where $\tilde{\mathbf{r}}$ is the signal after IN mitigation using CDA (in subsection III-A) and $\Lambda = \lfloor T_f/F_s \rfloor$ represents the total number of samples in a frame with F_s as the sampling frequency. Each $\tilde{\mathbf{r}}_i$ has time-aligned MPCs of MUI that are dynamic in nature from frame-to-frame. After averaging, received signal is expressed as $\hat{\mathbf{s}} = \frac{1}{N_f}\sum_{i=1}^{N_f} \tilde{\mathbf{r}}_i$. Averaging provides good MUI suppression at high SMUIR (signal-to-MUI ratio) and/or for large value of N_f. Thus, IN and MUI (impulsive interference) are mitigated in signal $\hat{\mathbf{s}}$. Next, $\hat{\mathbf{s}}$ is fed to the proposed non-coherent receiver for joint estimation of ToA and data symbols as shown in Fig. 1.

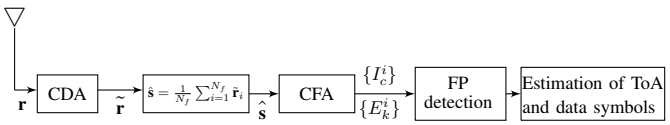

Fig. 1: Structure of the proposed non-coherent receiver for the joint estimation of ToA and data symbols in the presence of impulsive interference. CDA and averaging blocks mitigate impulsive interference present in the received signal $\mathbf{r}$. CFA provides the energy of UWB signal clusters and their peak valued time indices. Using $\{E_k^i\}$ and $\{I_c^i\}$, FP is detected that is subsequently used to estimate ToA and data symbols.

C. UWB signal cluster finding algorithm

Once IN and MUI are mitigated at the front end of the receiver using the proposed CDA and averaging technique, respectively, signal ($\hat{\mathbf{s}}$) can be used for ToA and data symbol estimation. The received UWB signal in a frame appears in the form of clusters. These clusters may be separated from each other. The conventional ED is not optimum because it also includes the non-signal portion (noise only) in the integration interval. Further, the starting and ending times of the integration in ED are not optimal (which needs CIR and noise information [18]). The proposed non-coherent receiver uses only the signal clusters and hence, enhances SNR at the receiver output by barring inter-cluster noise accumulation.

The signal $\hat{\mathbf{s}}$ (after CDA and averaging technique) is used to estimate the number of UWB signal clusters and their energy. These signal clusters in a frame are determined as follows: The maximum absolute peak value of signal $\hat{\mathbf{s}}$ and the corresponding time index are written as

$$[P^1_c, I^1_c] = \max(|\hat{\mathbf{s}}|). \quad (10)$$

First, cluster's center is located at I^1_c with an absolute peak value P^1_c in $\hat{\mathbf{s}}$. To find the next cluster in $\hat{\mathbf{s}}$, samples of signal $\hat{\mathbf{s}}$ for the cluster duration around the time index I^1_c are assigned zero values. This modified signal is used in (10) in place of $\hat{\mathbf{s}}$ to find the next cluster's center and maximum absolute peak value. This process is repeated until the peak value of a cluster decreases below a predefined '*X*' percentage of the first cluster's peak P^1_c. This provides the number of clusters (NOC) as

$$\text{NOC} = \max\left\{ i : |P^i_c| \geq \left| \frac{X \times P^1_c}{100} \right| \right\}, \quad i = 1, 2, ... \quad (11)$$

where P^1_c and P^i_c are the maximum absolute peak values of the first and the i^{th} cluster, respectively. Hence, '*X*' in (11) decides the number of signal clusters in the received signal.

Each UWB signal cluster has the same duration as the time width of the transmitted UWB pulse [18]. Since standardized

pulses are used [20], the type and time width of UWB pulse is known apriori in the system. Assuming a cluster width of $M+1$ samples (M is considered even without loss of generality) around the cluster peak, a cluster can be expressed as:

$$\mathbf{c}^i = \hat{\mathbf{s}}(I_c^i - M/2 : I_c^i + M/2),\ i = 1, 2, ..., \text{NOC}. \tag{12}$$

The energy of each cluster is calculated and expressed as $\tilde{E}_c^i = \sum_{m=1}^{M+1}(\mathbf{c}^i(m))^2$. The procedure of maximum absolute peak value based cluster finding algorithm (CFA) is also summarized in **Algorithm 1**. In the proposed receiver, each cluster energy is weighted using its peak value and is expressed as $E^i = P_c^i\ \tilde{E}_c^i,\ i = 1, 2, ..., \text{NOC}$. The proposed non-coherent receiver for the joint estimation of ToA and data symbols in the presence of impulsive interference is shown in Fig. 1. In Fig. 1, $\{E_k^i\}$ denotes the i^{th} cluster's energy for the k^{th} data symbol after IN and MUI mitigation.

Algorithm 1 CDA based IN mitigation and cluster finding algorithm (CFA)

CDA based IN mitigation:
Initialize: $\mu,\ M,\ i = 1$
Input: received signal $\mathbf{r}_i \in \mathbb{R}^N$
Output: estimated signal $\tilde{\mathbf{r}} \in \mathbb{R}^N$
Calculate: $[P_{max}^i, I_{max}^i] = \max(|\mathbf{r}_i|)$
Calculate: $\mathbf{c}_{in} = \mathbf{r}_i(I_{max}^i - M/2 : I_{max}^i + M/2)$
While: $\left(\sqrt{\sum_{n_m=1}^{M+1}\left(\mathbf{c}_{in}(n_m) - \mathbf{p}(n_m)\right)^2}\right) \geq \mu$
Update $\mathbf{r}_i = \mathbf{r}_i - \mathbf{e}_{I_{max}^i}\mathbf{r}_i$
Set $i = i + 1$
Calculate: $[P_{max}^i, I_{max}^i] = \max(|\mathbf{r}_i|)$
Calculate: $\mathbf{c}_{in} = \mathbf{r}_i(I_{max}^i - M/2 : I_{max}^i + M/2)$
End
Update $\tilde{\mathbf{r}} = \mathbf{r}_i$
Update: $\hat{\mathbf{s}} = \frac{1}{N_f}\sum_{i=1}^{N_f}\tilde{\mathbf{r}}_i$ (using (9) and averaging)

Cluster finding algorithm (CFA):

Initialize: $M,\ i = 1$, X, $\mathbf{O}_{1\times(M+1)}$- zero vector of size $1 \times (M+1)$
Input: Signal $\hat{\mathbf{s}}$
Output: $P_c^i,\ I_c^i,\ \tilde{E}_c^i$, NOC
$[P_c^i, I_c^i] = \max(|\hat{\mathbf{s}}|)$
While: condition in (11) is true
$\mathbf{c}^i = \hat{\mathbf{s}}(I_c^i - M/2 : I_c^i + M/2)$
$\tilde{E}_c^i = \sum_{m=1}^{M+1}(\mathbf{c}^i(m))^2$
Update $\hat{\mathbf{s}}(I_c^i - M/2 : I_c^i + M/2) = \hat{\mathbf{s}}(I_c^i - M/2 : I_c^i + M/2)\mathbf{O}_{1\times(M+1)}$
$\text{NOC} = i$
$i = i + 1$
$[P_c^i, I_c^i] = \max(|\hat{\mathbf{s}}|)$
Do

D. Joint estimation of ToA and data symbols

In this subsection, joint estimation of ToA and data symbols is proposed using $\{E^i, I_c^i\}_{i=1}^{\text{NOC}}$. E^1 represents cluster energy corresponding to the maximum valued MPC. Hence, ToA ($\tau_{toa,mep}$) based on MEP is given by

$$\tau_{toa,mep} = I_c^1\ t_s, \tag{13}$$

where t_s ($t_s = 1/F_s$) is the sampling time interval. However, I_c^1 may not necessarily represent the time index of FP of the received signal because FP may not have maximum energy. For example, in Fig. 2, MEP is not the FP. Hence, time index I_c^1 is not the correct arrival time of FP that subsequently leads to higher UWB ranging error. In order to detect FP accurately, an iterative refinement in cluster time indices is carried out. Let $I_{fp} = I_c^1$ and I_c^2 represents the time index of second MEP (E^2). If $I_c^2 < I_{fp}$, then $I_{fp} = I_c^2$; else I_{fp} remains unchanged. The same process is repeated ((NOC-1) times) for other clusters. In the end, I_{fp} represents the FP time index. In Fig. 2, iterative refinement is repeated three times to obtain the FP time index and hence, $I_{fp} = I_c^4$. Thus, estimation of ToA of FP is expressed as

$$\hat{\tau}_{toa} = I_{fp}\ t_s. \tag{14}$$

If we assume that the k^{th} frame contains the data symbol d_k, then $\tau_1 = \hat{\tau}_{\text{toa}} + d_k\Delta$. Data symbols are demodulated using $\hat{\tau}_{toa}$ and PPM index Δ, and are expressed as

$$\hat{d}_k = \frac{\tau_1 - \hat{\tau}_{toa}}{\Delta}. \tag{15}$$

E. FP detection error probability

FP detection depends on clusters' energy, where clusters are formed around the maximum absolute peak valued samples in $\hat{\mathbf{s}}$. Therefore, if a cluster is selected corresponding to noise only (and not due to presence of the desired signal plus noise), it leads to detection error probability in ToA estimation. Signal $\hat{\mathbf{s}}$ in a single cluster duration is expressed as

$$\begin{aligned} \mathcal{H}_{\tilde{\mathbf{n}}} &: \hat{\mathbf{s}} = \tilde{\mathbf{n}} \in \mathbb{R}^{M+1}, \\ \mathcal{H}_{\hat{\mathbf{c}}} &: \hat{\mathbf{s}} = \mathbf{s} + \tilde{\mathbf{n}} \in \mathbb{R}^{M+1}, \end{aligned} \tag{16}$$

where $\tilde{\mathbf{n}}$ ($\tilde{\mathbf{n}} \sim \mathcal{N}(0, \sigma_{\tilde{n}}^2)$) represents noise in $\hat{\mathbf{s}}$ after impulsive interference mitigation and may be different from $\mathbf{n}$. Hypotheses $\mathcal{H}_{\tilde{\mathbf{n}}}$ and $\mathcal{H}_{\hat{\mathbf{c}}}$ represent clusters corresponding to noise-only and signal plus noise, respectively. Let $\pi_{\mathcal{H}_{\tilde{\mathbf{n}}}}$ and $\pi_{\mathcal{H}_{\hat{\mathbf{c}}}}$ be the probabilities of hypotheses $\mathcal{H}_{\tilde{\mathbf{n}}}$ and $\mathcal{H}_{\hat{\mathbf{c}}}$ respectively. The distribution of energy ($E_{\hat{\mathbf{s}}} = \sum_{i=1}^{M+1}\hat{\mathbf{s}}(i)^2$) of single cluster duration is given as

$$\begin{aligned} &\mathcal{N}(\sigma_{\tilde{n}}^2(M+1), \sigma_{\tilde{n}}^4(M+1)) \quad \text{under } \mathcal{H}_{\tilde{\mathbf{n}}}, \\ &\mathcal{N}\left((\sigma_s^2 + \sigma_{\tilde{n}}^2)(M+1), (2\sigma_s^2\sigma_{\tilde{n}}^2 + \sigma_{\tilde{n}}^4)(M+1)\right) \quad \text{under } \mathcal{H}_{\hat{\mathbf{c}}}, \end{aligned} \tag{17}$$

where σ_s^2 is the variance of $\mathbf{s}$. Probability distribution in (17) is approximated form of Chi-square distributed energy ($E_{\hat{\mathbf{s}}}$) and an approximation is close to actual distribution for $M \geq 10$ [21, 22]. The MEP based error probability of FP detection p_{fp} of ToA estimation can be expressed as

$$\begin{aligned} p_{\text{fp}} &= \pi_{\mathcal{H}_{\tilde{\mathbf{n}}}}\ Pr\{E_{\hat{\mathbf{s}}}|\mathcal{H}_{\tilde{\mathbf{n}}} > E_{\hat{\mathbf{s}}}|\mathcal{H}_{\hat{\mathbf{c}}}\} + \pi_{\mathcal{H}_{\hat{\mathbf{c}}}}\ Pr\{E_{\hat{\mathbf{s}}}|\mathcal{H}_{\tilde{\mathbf{n}}} > E_{\hat{\mathbf{s}}}|\mathcal{H}_{\hat{\mathbf{c}}}\} \\ &= \pi_{\mathcal{H}_{\tilde{\mathbf{n}}}}\ Pr\{E_{\hat{\mathbf{s}}}|\mathcal{H}_{\tilde{\mathbf{n}}} - E_{\hat{\mathbf{s}}}|\mathcal{H}_{\hat{\mathbf{c}}} > 0\} + \pi_{\mathcal{H}_{\hat{\mathbf{c}}}}\ Pr\{E_{\hat{\mathbf{s}}}|\mathcal{H}_{\tilde{\mathbf{n}}} - E_{\hat{\mathbf{s}}}|\mathcal{H}_{\hat{\mathbf{c}}} > 0\}. \end{aligned} \tag{18}$$

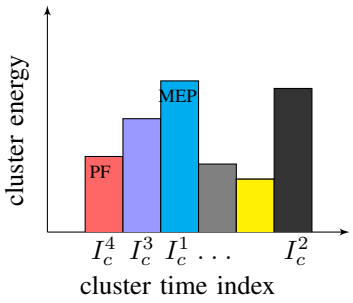

Fig. 2: Plot of Clusters' energy and their time indices; Time indices I_c^1 and I_c^4 represent MEP and FP clusters, respectively.

After mathematical simplifications, $p_{\mathrm{f}p}$ is written as $p_{\mathrm{f}p} = (\pi_{\mathcal{H}_{\tilde{\mathbf{n}}}} + \pi_{\mathcal{H}_{\hat{\mathbf{c}}}})\, Q\left(\frac{(M+1)\sigma_s^2}{\sqrt{2\sigma_{\tilde{n}}^2(\sigma_s^2+\sigma_{\tilde{n}}^2)(M+1)}}\right)$. Further, $p_{\mathrm{f}p}$ is approximated at high SNR ($\pi_{\mathcal{H}_{\hat{\mathbf{c}}}} >> \pi_{\mathcal{H}_{\tilde{\mathbf{n}}}}$ and $\sigma_s^2 >> \sigma_{\tilde{n}}^2$) as $p_{\mathrm{f}p} = Q\left(\sqrt{\frac{M\sigma_s^2}{2\sigma_{\tilde{n}}^2}}\right)$.

In (18), $\pi_{\mathcal{H}_{\tilde{\mathbf{n}}}}$ is calculated as $Pr\{\max\{|s+\tilde{n}|, |\tilde{n}|\} = |\tilde{n}|\}$. Further, let $\xi = \max\{|s+\tilde{n}|, |\tilde{n}|\}$ and can written as $\xi = \frac{1}{2}\left(|s| + |s+2\tilde{n}|\right)$. Therefore,

$$\begin{aligned}\pi_{\mathcal{H}_{\tilde{\mathbf{n}}}} &= Pr\{\xi | s>0, \tilde{n}<0, s<-2\tilde{n}\} + Pr\{\xi | s<0, \tilde{n}>0, s>-2\tilde{n}\} \\ &= Pr\{-\tilde{n} | s>0, \tilde{n}<0, s<-2\tilde{n}\} + Pr\{\tilde{n} | s<0, \tilde{n}>0, s>-2\tilde{n}\} \\ &= f_{\tilde{n}}(-\xi),\ \xi \geq 0, \xi > s/2, s>0 + f_{\tilde{n}}(\xi),\ \xi \geq 0, \xi > -s/2, s<0,\end{aligned} \tag{19}$$

where $f_{\tilde{n}}(\tilde{n})$ is the pdf of $\tilde{n}$ and finally

$$\begin{aligned}\pi_{\mathcal{H}_{\tilde{\mathbf{n}}}} &= Q\left(\frac{s/2}{\sqrt{\sigma_{\tilde{n}}^2}}\right),\ s>0 + Q\left(\frac{-s/2}{\sqrt{\sigma_{\tilde{n}}^2}}\right),\ s<0 \\ &= Q\left(\sqrt{\frac{s^2}{4\sigma_{\tilde{n}}^2}}\right), \forall s\end{aligned} \tag{20}$$

The value of $\pi_{\mathcal{H}_{\tilde{\mathbf{n}}}} \to 0$ as SNR increases and $\pi_{\mathcal{H}_{\hat{\mathbf{c}}}} = 1 - \pi_{\mathcal{H}_{\tilde{\mathbf{n}}}}$.

The value of 'X' in (11) is chosen such that all dominant clusters of signal $\hat{\mathbf{s}}$ are selected. Large values of 'X' may miss few signal clusters, while small values of 'X' may select clusters in the noise-only region too. The dominant energy signal clusters appear at the start of the frame [23], while clusters due to noise-only region mostly belong to the later part of a frame. The proposed method first selects the maximum energy cluster, which is partially independent of the exact number of clusters (because maximum energy cluster is selected first in the proposed receiver design). Based on the empirical results, the value of 'X' can be selected between 10% to 20%. Therefore, the marginal change in the total number of clusters does not affect the performance of the proposed receiver.

IV. Numerical Results

In this section, numerical results are discussed to validate the proposed non-coherent receiver design for the joint estimation of ToA and data symbols. The transmitted UWB pulse ($\mathbf{p}$) is the normalized second derivative Gaussian pulse of duration around 0.8 nanoseconds (ns) [4, 9]. In simulations, sampling frequency is 16 GHz and TH code is generated as in [11, 17, 18]. Each interferer and the desired user utilize the same BPPM scheme and the same UWB pulse. Further, $N_f = 5$, $U = 5$, $p = 0.01$, SIR $= -40$ dB, and $T_f = 200$ ns are considered. The frame level synchronization between the transmitter and receiver is required only in the proposed non-coherent UWB receiver. The legend "CFA (G)" represents the proposed CFA based receiver's performance in the presence of Gaussian noise only.

Fig. 3 shows the received signal ($\mathbf{r}$), the CDA output ($\tilde{\mathbf{r}}$), and the desired multipath UWB signal ($\mathbf{s}$). In this simulation, MUI $= 0$, SNR $= 30$ dB, and two frame time duration signal lengths are considered in IEEE 802.15.4a multipath CM1 channel [24]. The desired UWB signal is completely buried within the sparse high amplitude IN as observed in Fig. 3 (a). Therefore, conventional receiver does not work (or have high error rate) in the presence of IN. The IN is mitigated using the proposed CDA without changing the desired UWB signal as shown in Fig. 3 (b). The proposed CDA need not require any threshold. Hence, it also works in the absence of prior knowledge of IN.

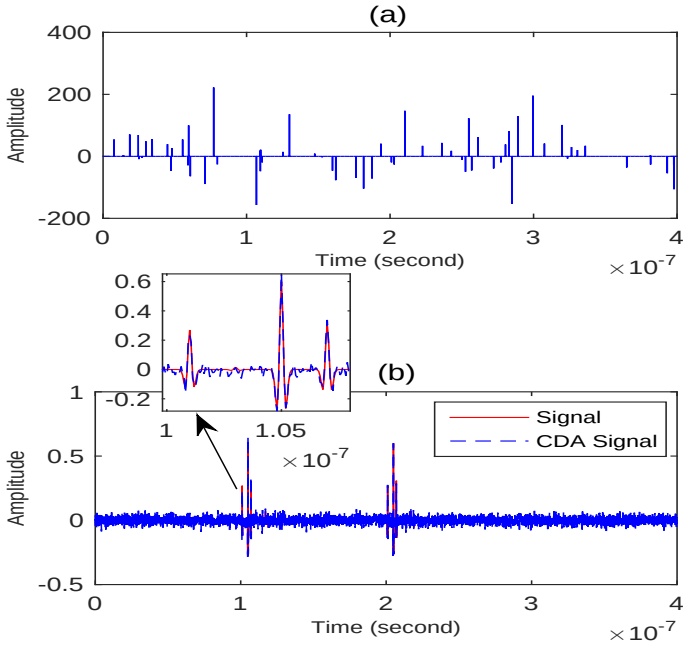

Fig. 3: Received signal (top) and CDA output (bottom) using $p = 0.01$, SIR $= -40$ dB, and SNR $= 30$ dB. After IN mitigation, CDA output signal ("CDA Signal") and true signal ("Signal") are same (as shown in zoom portion).

Next, MUI is mitigated (or minimized) using the proposed method utilizing different TH codes and signal averaging. The MUI and desired signal are shown in Fig. 4. The MUI is differently time-aligned in each frame, while the desired signal has the same time alignment as observed in Fig. 4. The MPCs of MUI can be separated from the desired signal due to different TH codes from frame to frame. The desired signal has the same signal strength and time alignment in each

frame (across N_f consecutive frames). Hence, by averaging the signal over N_f frames, MUI effect is mitigated without requiring the knowledge of the TH codes of interferers.

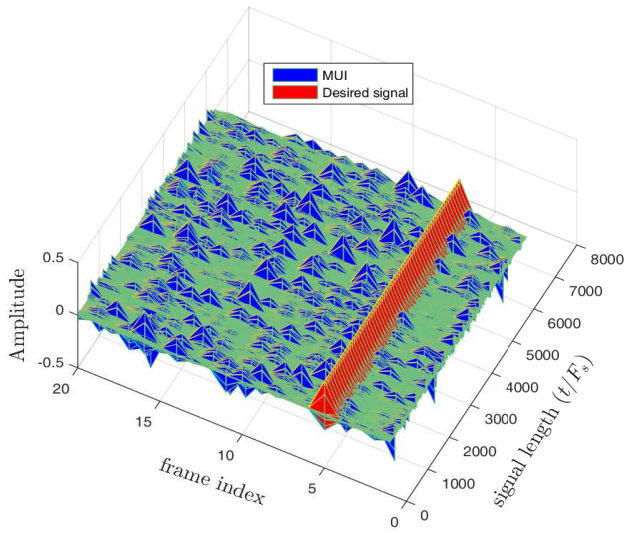

Fig. 4: Effective de-hopping of impulse responses over CM1 channel using $N_f = 20$ and U=5.

The average ToA error and bit error rate (BER) using the proposed non-coherent receiver in the presence of IN (MUI = 0) are evaluated in IEEE 802.15.4a CM1 channel [24]. The root mean square error (RMSE) between the estimated and the true ToA of FP is calculated as RMSE $= \sqrt{(\hat{\tau}_{toa} - \tau_1)^2}$ and is shown in Fig. 5. The MEP based RMSE using ED (with integration interval 1 ns) and the proposed CFA based receiver (in short CFAR) in the presence of IN is denoted as "ED (MEP)" and "CFA (MEP)", respectively, in Fig. 5. CFAR performs better than ED as observed in Fig. 5. Legends "CFA" and "CFA (G)" denote the CFAR performance in IN and Gaussian noise, respectively, using (14), and both are observed to have the same performance. Further, TC based ED performance using the normalized threshold [5] and the mean value based threshold is evaluated in Gaussian noise. These are labeled in Fig. 5 as "TC, norm (G)" and "TC, mean (G)", respectively. To find the normalized and mean valued based threshold, exact noise and signal statistics such as power are required to be calculated at each SNR. This is generally difficult (or complex) in practice. Therefore, threshold based methods are either inappropriate or lead to large ranging error in the absence of prior knowledge of noise. Further, CFAR performs better than TC based ED at high SNR as shown in Fig. 5 and does not require any threshold.

The average BER performance of BPPM UWB system using (15) is shown in Fig. 6 in the presence of IN and Gaussian noise. ED exhibits bit error floor at high SNR region in the presence of IN as observed in Fig. 6. CFAR is free from any bit error floor in IN, but its performance degrades around 5 dB at BER $= 10^{-4}$ similar to ED as compared to Gaussian noise only ("CFA(G)" in Fig. 6). Further, CFAR performs better than ED in Gaussian noise only as shown in Fig. 6. Hence, improved performance of CFAR is observed as compared to ED in both IN and Gaussian noise scenarios.

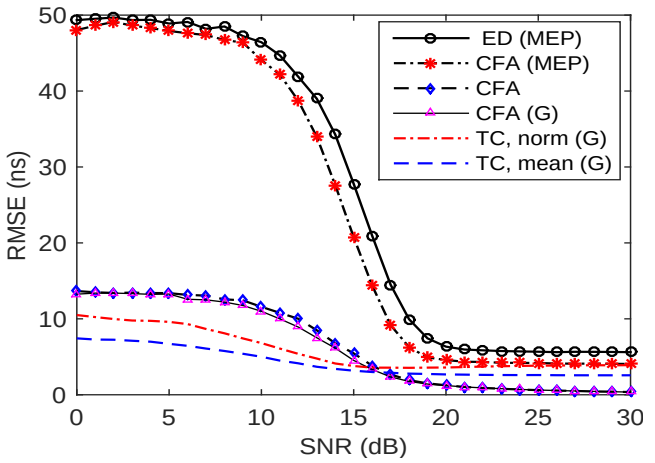

Fig. 5: Average RMSE of ToA estimation in the presence of Gaussian (G) and IN scenarios. The RMSE performance of MEP and TC based ED, and proposed CFA based receiver are compared.

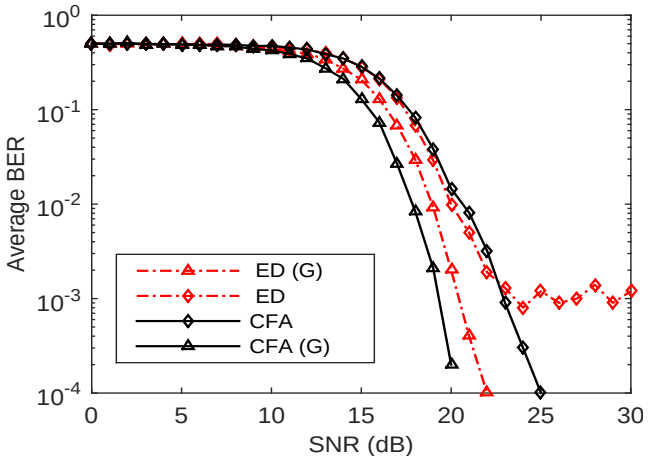

Fig. 6: Average BER performance of BPPM UWB system using (15) in the presence of Gaussian noise only ("X(G)") and both IN and Gaussian noise ("X"). Here, X stands for either ED or CFA.

Further, joint estimation of ToA and data symbols is carried out in the presence of both IN and MUI scenario. First, we mitigate IN and MUI from the received signal using the proposed CDA and the averaging technique, respectively. RMSE results of ToA and BER using CFAR are shown in Fig. 7. RMSE in the presence of both IN and MUI is slightly higher (around 1.5 ns) in 10 dB to 20 dB SNR range. However, at high SNR, RMSE is same for all scenarios as observed in Fig. 7 (top). The average BER performance of BPPM UWB system using (15) in the presence of Gaussian, MUI, IN, and both MUI and IN is shown Fig. 7 (bottom). In the presence of MUI, BER degrades in high SNR region due to the non-zero flooring of MUI as observed in Fig. 7 (bottom). However, providing different TH code to each interferer or a large value

of N_f (but confined due to coherence time of CIR), we can reduce the flooring of MUI. Further, BER degrades around 5 dB at BER $= 10^{-4}$ due to IN as compared to the Gaussian noise only case as noted from Fig. 7 (bottom).

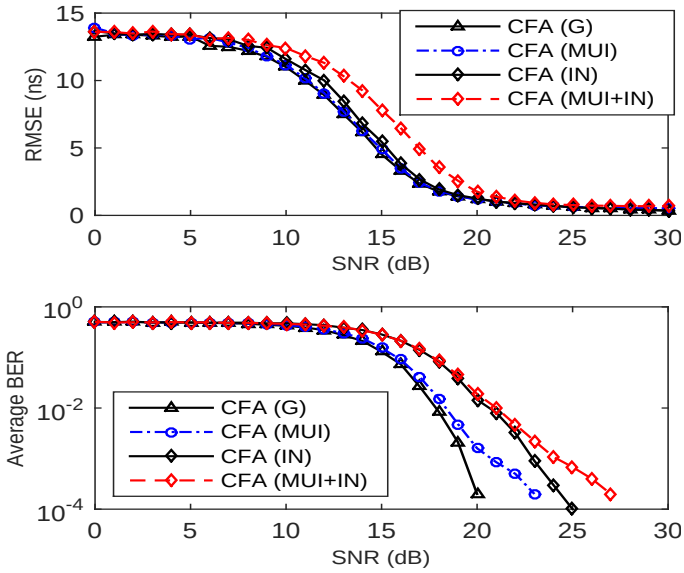

Fig. 7: The joint estimation of ToA and data symbols in the presence of Gaussian ("CFA (G)"), MUI ("CFA (MUI)"), IN ("CFA (IN)"), and both MUI and IN ("CFA (MUI+IN)") using the proposed CFA based receiver over the multipath CM1 channel.

V. Conclusion

In this paper, a robust non-coherent UWB receiver is proposed for impulsive interference scenario. The proposed receiver successfully mitigates the impulsive interference from the received signal. After, impulsive interference mitigation, the proposed cluster finding algorithm is employed that provides better ranging and bit error rate performance as compared to the conventional energy detection based receiver. Further, the proposed receiver is free from threshold value selection in both the impulsive interference mitigation and the time-of-arrival estimation stages, unlike conventional receivers. Hence, the proposed receiver is suitable when prior knowledge is not adequate to determine the optimal detection threshold. In the near future, the performance of the proposed receiver will be analyzed for other modulation schemes and for coherent detection in UWB communication.

Acknowledgement

The authors would like to thank Visvesvaraya Ph.D. scheme of the Ministry of Electronics and Information Technology (Meity), Govt. of India, IIT Indore and IIIT Delhi for all the support.

References

[1] D. Dardari, A. Conti, U. Ferner, A. Giorgetti, and M. Z. Win, "Ranging with ultrawide bandwidth signals in multipath environments," *IEEE Proceedings*, vol. 97, no. 2, pp. 404–426, 2009.

[2] V. Kristem, A. F. Molisch, S. Niranjayan, and S. Sangodoyin, "Coherent UWB ranging in the presence of multiuser interference," *IEEE Transactions on Wireless Communications*, vol. 13, no. 8, pp. 4424–4439, 2014.

[3] I. Guvenc, Z. Sahinoglu, and P. V. Orlik, "TOA estimation for IR-UWB systems with different transceiver types," *IEEE Transactions on Microwave Theory and Techniques*, vol. 54, no. 4, pp. 1876–1886, 2006.

[4] H. Ding, W. Liu, X. Huang, and L. Zheng, "First path detection using rank test in IR UWB ranging with energy detection receiver under harsh environments," *IEEE Communications Letters*, vol. 17, no. 4, pp. 761–764, 2013.

[5] I. Guvenc and Z. Sahinoglu, "Threshold-based TOA estimation for impulse radio UWB systems," in *IEEE International Conference on Ultra-Wideband*, 2005, pp. 420–425.

[6] H. Cai, T. Lv, H. Gao, A. Hu, and Y. Lu, "An optimized first path detector for UWB ranging using error characteristics," in *IEEE Wireless Communications and Networking Conference (WCNC)*, 2014, pp. 1230–1235.

[7] W. Liu, H. Ding, X. Huang, and Z. Liu, "TOA estimation in IR UWB ranging with energy detection receiver using received signal characteristics," *IEEE Communications Letters*, vol. 16, no. 5, pp. 738–741, 2012.

[8] A. Giorgetti and M. Chiani, "Time-of-arrival estimation based on information theoretic criteria," *IEEE Transactions on Signal Processing*, vol. 61, no. 8, pp. 1869–1879, 2013.

[9] S. Sharma, V. Bhatia, and A. Gupta, "Sparsity based UWB receiver design in additive impulse noise channels," in *IEEE 17th International Workshop on Signal Processing Advances in Wireless Communications (SPAWC)*, 2016, pp. 1–5.

[10] D. Dardari, A. Giorgetti, and M. Z. Win, "Time-of-arrival estimation of UWB signals in the presence of narrowband and wideband interference," in *IEEE International Conference on Ultra-Wideband (ICUWB)*, 2007, pp. 71–76.

[11] S. Sharma, V. Bhatia, and A. Gupta, "Sparsity-based narrowband interference mitigation in ultra wide-band communication for 5G and beyond," *Computers & Electrical Engineering*, vol. 3, pp. 1–13, 2017.

[12] Y. Dhibi and T. Kaiser, "Impulsive noise in UWB systems and its suppression," *Mobile Networks and Applications*, vol. 11, no. 4, pp. 441–449, 2006.

[13] F. Yin, C. Fritsche, F. Gustafsson, and A. M. Zoubir, "TOA-based robust wireless geolocation and Cramér-Rao lower bound analysis in harsh LOS/NLOS environments," *IEEE Transactions on Signal Processing*, vol. 61, no. 9, pp. 2243–2255, 2013.

[14] F. Shang, B. Champagne, and I. Psaromiligkos, "Joint TOA/AOA estimation of IR-UWB signals in the presence of multiuser interference," in *IEEE 15th International Workshop on Signal Processing Advances in Wireless Communications (SPAWC)*, 2014, pp. 504–508.

[15] H. Oh and H. Nam, "Design and performance analysis of non-linearity preprocessors in an impulsive noise environment," *IEEE Transactions on Vehicular Technology*, vol. PP, no. 99, 2016.

[16] N. Güney, H. Deliç, and M. Koca, "Robust detection of ultra-wideband signals in non-Gaussian noise," *IEEE Transactions on Microwave Theory and Techniques*, vol. 54, no. 4, pp. 1724–1730, Apr. 2006.

[17] Q. Zhou and X. Ma, "Receiver designs for differential UWB systems with multiple access interference," *IEEE Transactions on Communications*, vol. 62, no. 1, pp. 126–134, 2014.

[18] S. Sharma, V. Bhatia, and A. Gupta, "A non-coherent UWB receiver using signal cluster sparsity," in *IEEE 23rd National Conference on Communication (NCC)*, March 2017, pp. 1–6.

[19] B. Li, C. Zhao, H. Zhang, X. Sun, and Z. Zhou, "Characterization on clustered propagations of UWB sensors in vehicle cabin: measurement, modeling and evaluation," *IEEE Sensors Journal*, vol. 13, no. 4, pp. 1288–1300, 2013.

[20] N. C. Beaulieu and B. Hu, "On determining a best pulse shape for multiple access ultra-wideband communication systems," *IEEE Transactions on Wireless Communications*, vol. 7, no. 9, 2008.

[21] K. Arshad, M. A. Imran, and K. Moessner, "Collaborative spectrum sensing optimisation algorithms for cognitive radio networks," *International Journal of Digital Multimedia Broadcasting*, vol. 2010, 2010.

[22] P. K. Varshney, *Distributed detection and data fusion*. Springer Science & Business Media, 2012.

[23] S. Sharma, A. Gupta, and V. Bhatia, "A new sparse signal-matched measurement matrix for compressive sensing in UWB communication," *IEEE Access*, vol. 4, pp. 5327–5342, 2016.

[24] A. F. Molisch, D. Cassioli, C.-C. Chong, S. Emami, A. Fort, B. Kannan, J. Karedal, J. Kunisch, H. G. Schantz, K. Siwiak *et al.*, "A comprehensive standardized model for ultrawideband propagation channels," *IEEE Transactions on Antennas and Propagation*, vol. 54, no. 11, pp. 3151–3166, 2006.